Journal of Differential Equations **168**, 150–167 (2000)
doi:10.1006/jdeq.2000.3882, available online at http://www.idealibrary.com on IDEAL®

Homoclinic Bifurcation in an *SIQR* Model for Childhood Diseases

Lih-Ing Wu[1] and Zhilan Feng[2]

Department of Mathematics, Purdue University, West Lafayette, Indiana 47907

Received August 31, 1999; revised February 22, 2000

DEDICATED TO PROFESSOR JACK HALE ON THE OCCASION OF HIS 70TH BIRTHDAY

We consider a system of ODEs which describes the transmission dynamics of childhood diseases. A center manifold reduction at a bifurcation point has the normal form $x' = y$, $y' = axy + bx^2y + O(4)$, indicating a bifurcation of codimension greater than two. A three-parameter unfolding of the normal form is studied to capture possible complex dynamics of the original system which is subjected to certain constraints on the state space due to biological considerations. It is shown that the perturbed system produces homoclinic bifurcation. © 2000 Academic Press

1. INTRODUCTION

In *Feng and Thieme* [5] an *SIQR* model for childhood diseases (a system of ODEs) is formulated to study the impact of isolation on the observed periodic occurrence of these diseases. They show that if the average length of the isolation period is either very long or very short the disease dynamics always converge to the endemic equilibrium (global stability). Analytically they have found two different parameter values at which periodic solutions bifurcate from the endemic equilibrium via a Hopf bifurcation. Their numerical studies using *Auto* show that for parameter values in a certain range, the branches of periodic solutions emanating at these two bifurcation points are disconnected and periods of these solutions tend to infinity, suggesting the presence of homoclinic orbits.

In this article we derive an analytic understanding of the complex dynamics that may arise from the *SIQR* model. Using tools in dynamical systems theory such as center manifold reduction, normal form, and unfolding methods we show that homoclinic bifurcation exists in a biologically reasonable region of the parameter and state space.

The vector field of our model equations has a singularity of codimension greater than two for some critical parameter values. This is indicated by the

[1] E-mail: wuli@math.purdue.edu.
[2] E-mail: zfeng@math.purdue.edu.

0022-0396/00 $35.00

fact that the normal form of a center manifold reduction of the full system (near a threshold) has the form

$$\begin{aligned} \dot{x} &= y, \\ \dot{y} &= bxy + \beta x^2 y + O(4), \end{aligned} \tag{1.1}$$

where $O(n)$ denotes all monomial terms of degree n and higher. In [1], the second order normal form

$$\begin{aligned} \dot{x} &= y, \\ \dot{y} &= ax^2 + bxy, \qquad a \neq 0, \end{aligned} \tag{1.2}$$

was studied, and a complete bifurcation analysis of (1.2) with a two-parameter unfolding given by the Takens–Bogdanov system

$$\begin{aligned} \dot{x} &= y, \\ \dot{y} &= \mu_1 x + \mu_2 y + x^2 \pm xy, \end{aligned} \tag{1.3}$$

can be found in [2, 6]. If $b \neq 0$, it is a cusp of codimension 2; if $b = 0$, it is a cusp of higher codimension. There are also results for the case of $a = 0$ and $b \neq 0$ in (1.2), but with some higher order terms included. For example, the following order three normal form

$$\begin{aligned} \dot{x} &= y, \\ \dot{y} &= bxy + \alpha x^3 + \beta x^2 y, \qquad \alpha \neq 0, \end{aligned} \tag{1.4}$$

has a universal unfolding with three parameters

$$\begin{aligned} \dot{x} &= y, \\ \dot{y} &= \mu_1 + \mu_2 x + y(\mu_3 + bx + \beta x^2) + \alpha x^3, \end{aligned} \tag{1.5}$$

which is presented in [4].

We see that our normal form (1.1) is highly degenerate in the sense that the corresponding coefficients a in (1.2) and α in (1.3) are both zero. To our knowledge, no universal unfolding of normal forms of type (1.1) has been found. However, this is not our goal. We do not wish to obtain complete bifurcation analysis of (1.1). In fact, since our equations are from an epidemic model, there are some constraints on the state and parameter space. For example, the solutions that represent numbers of individuals cannot be negative. These restrictions rule out unfoldings that produce biologically unreasonable solutions.

The purposes of this paper are quite specific. We study the *SIQR* model through unfolding analysis of a normal form derived from the model

equations. In particular, we find an unfolding which gives rise to a codimension two bifurcation as well as limit cycles and homoclinic orbits as expected from previous numerical studies. The results are proved analytically. We also show some numerical computations to confirm the existence of Hopf and homoclinic bifurcations. The behaviors of the simplified system will then represent the different dynamics which may occur for the original system under small perturbations.

The paper is organized as follows. In Section 2 we explain the *SIQR* model, describe its basic dynamics, and compute a center manifold reduction of the equations at a critical point and a normal form of the reduced system. Section 3 presents an unfolding of the normal form and its bifurcation analysis. Some numerical computations are also included in this section. Section 4 discusses the results.

2. THE *SIQR* MODEL AND SINGULARITIES OF THE VECTOR FIELD

The following model for childhood disease is proposed in [5]:

$$\begin{aligned}
\frac{d}{dt} S &= \Lambda - \mu S - \sigma S \frac{I}{A}, \\
\frac{d}{dt} I &= -(\mu + \gamma) I + \sigma S \frac{I}{A}, \\
\frac{d}{dt} Q &= -(\mu + \xi) Q + \gamma I, \\
\frac{d}{dt} R &= -\mu R + \xi Q, \\
A &= S + I + R.
\end{aligned} \tag{2.1}$$

S, I, Q, R denote the number of susceptible, infected, isolated (quarantined), and recovered individuals, respectively. A is the active; i.e., non-isolated individuals. Λ is the rate at which individuals are born into the population; μ is the per capita mortality rate; σ is the per capita infection rate of an average susceptible individual provided that everybody else is infected; γ is the rate at which individuals leave the infective class, and ξ is the rate at which individuals leave the isolated class; they are all positive constants.

Let $N = S + I + Q + R$ denote the total population. Note that $\frac{d}{dt} N = \Lambda - \mu N$, and $N(t) \to \Lambda/\mu$ as $t \to \infty$. By assuming that the size of the population has reached its limiting value; i.e., $N \equiv \Lambda/\mu \equiv S + I + Q + R = A + Q$, and using

$A = N - Q$ and $S = A - I - R$ in (2.1) we can eliminate S from the equations. Further we can introduce the fractions $u = \frac{S}{A}$, $p = \frac{I}{A}$, $q = \frac{Q}{A}$, $z = \frac{R}{A}$, and scale time such that $\sigma = 1$ by introducing a new, dimensionless, time $\tau = \sigma t$. This gives us the simplified system

$$\begin{aligned} \dot{p} &= p(1 - \nu - \theta - p - z + \theta p - (\nu + \zeta)\, q), \\ \dot{q} &= (1 + q)(\theta p - (\nu + \zeta)\, q), \\ \dot{z} &= \zeta q - \nu z + z(\theta p - (\nu + \zeta)\, q), \end{aligned} \tag{2.2}$$

where $\nu = \frac{\mu}{\sigma}$, $\theta = \frac{\gamma}{\sigma}$, and $\zeta = \frac{\xi}{\sigma}$. Here we have used the fact that $u = 1 - p - z$. It can be shown that the region

$$D = \{(p, q, z) \mid 0 \leqslant p \leqslant 1,\ q \geqslant 0,\ 0 \leqslant z \leqslant 1\} \tag{2.3}$$

is invariant.

The dynamics of (2.2) is dependent on the quantity $\mathscr{R}_0 = 1/(\nu + \theta)$ which, in biological terms, is called the *basic reproductive number*. The following results are proved in [5].

(1) If $\mathscr{R}_0 < 1$, then system (2.2) has only the trivial (disease-free) equilibrium $E_0 = (p_0, q_0, z_0) = 0$ which is globally asymptotically stable. If $\mathscr{R}_0 > 1$, then E_0 is unstable, and there exists a unique non-trivial (endemic) equilibrium $E^* = (p^*, q^*, z^*)$ with $p^* > 0$.

(2) If the quarantine period $(1/\zeta)$ is very short or very long, E^* attracts all solutions of system (2.2) with nonnegative initial data such that $p_0 > 0$.

(3) There exist ζ_0 and ζ_1 $(\zeta_0 < 1\zeta_1)$ such that E^* is locally asymptotically stable if $\zeta < 1\zeta_0$ or $\zeta > \zeta_1$, and E^* is unstable if $\zeta > \zeta_0$ and $\zeta > \zeta_1$. Hopf bifurcations occur at ζ_0 and ζ_1.

Calculations with Doedel's program *Auto* [3] show that the Hopf bifurcation is supercritical at both bifurcation points for parameters in a certain biologically reasonable region (see Fig. 1). We also observed that, for parameters in some other regions, when ζ moves away from ζ_1, the period of the periodic solution increases dramatically until the numerical methods fail to work properly. Can we derive an analytical understanding of the possible complex dynamics arising from this epidemic model?

Note that important disease dynamics of the model can be determined by the threshold $\mathscr{R}_0 = 1$, where $\mathscr{R}_0 = 1/(\nu + \theta)$ and $\nu = \mu/\sigma$, $\theta = \gamma/\sigma$. Also note that $\mu = 1/L$ with L denoting the average life expectation of humans, and $1/\gamma$ is the length of the infective period. The life span is on the order of decades whereas the infective period is on the order of days. Hence μ is much smaller than γ, and so ν is much smaller than θ. This leads us to choose the parameter values $\nu = 0$,

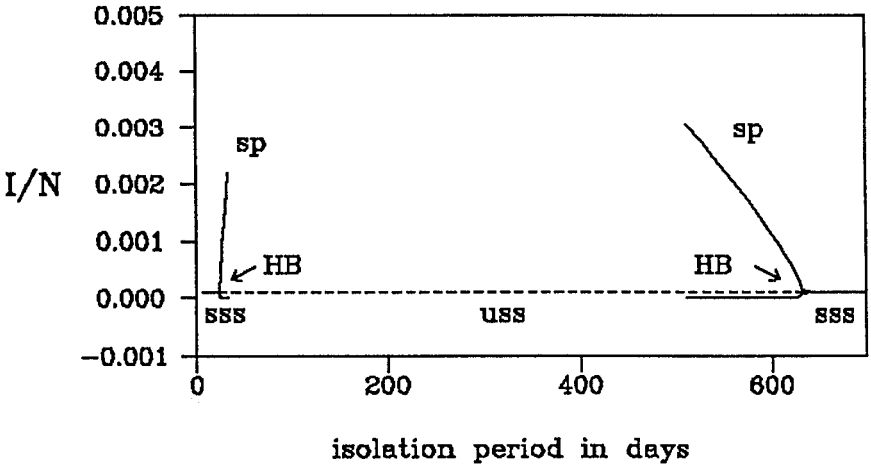

FIG. 1. An Auto plot of the lower and upper amplitudes of the periodic solutions (in terms of the fraction I/N) versus the length of the isolation period $1/\xi$. *HB* denotes Hopf bifurcation point, *sss* means (locally asymptotically) stable steady state, *uss* means unstable steady state, and *sp* is the (locally asymptotically orbitally) stable periodic solution.

$\theta = 1$ at the threshold $\mathscr{R}_0 = 1$, and consider the corresponding system as an approximation of the original system.

THEOREM 2.1. *The vector field* (2.2) *at the point* $v = 0, \theta = 1$ *has a singularity of codimension greater than two.*

In order to prove the theorem we need to introduce some notations and the normal form theorem. Let H_2 denote the linear space of vector fields whose coefficients are homogeneous polynomials of degree 2, $J = \left(\begin{smallmatrix} 0 & 1 \\ 0 & 0 \end{smallmatrix}\right)$, and

$$L_J(\tilde{h}(\mathbf{x})) \equiv -(D\tilde{h}(\mathbf{x})\, J\mathbf{x} - J\tilde{h}(\mathbf{x})),$$

where $\mathbf{x} \in \mathbf{R}^2$, $\tilde{h}$: $\mathbf{R}^2 \to \mathbf{R}^2$, and L_J: $H_2 \to H_2$. Choose a complementary G_2 for $L_J(H_2)$ in H_2, so that $H_2 = L_J(H_2) \oplus G_2$. The following theorem is taken from [8] (for the case of $r = 2$).

NORMAL FORM THEOREM. *By an analytic coordinate change* $\mathbf{x} = \mathbf{y} + \tilde{h}(\mathbf{y})$; *the system*

$$\mathbf{x}' = J\mathbf{x} + F_2(\mathbf{x}) + O(|\mathbf{x}|^3)$$

can be transformed into

$$\mathbf{y}' = J\mathbf{y} + \tilde{F}_2(\mathbf{y}) + O(|\mathbf{y}|^3),$$

where $\tilde{F}_2(y) \in G_2$.

From the above theorem, we can choose $\tilde{h}(\mathbf{y})$ such that only $O(|\mathbf{y}|^2)$ terms that are in G_2 remain. In the new coordinate system, only second order terms are in a space complementary to $L_J(H_2)$.

Proof of Theorem 2.1. When $v=0$, $\theta=1$ (2.2) becomes

$$\begin{aligned}\dot{p} &= p(-z-\zeta q),\\ \dot{q} &= (1+q)(p-\zeta q),\\ \dot{z} &= \zeta q + z(p-\zeta q).\end{aligned} \tag{2.4}$$

The system (2.4) has one negative and double zero eigenvalues at the equilibrium $e_0=(p_0, q_0, z_0)=(0, 0, 0)$. By the linear transformation

$$\begin{pmatrix} p\\ q\\ z\end{pmatrix} = \begin{pmatrix} 0 & \zeta & 0\\ 0 & 1 & 1\\ \zeta & 0 & -1\end{pmatrix}\begin{pmatrix} u\\ v\\ w\end{pmatrix} \tag{2.5}$$

the system (2.4) can be transformed into

$$\begin{pmatrix} \dot{u}\\ \dot{v}\\ \dot{w}\end{pmatrix} = \begin{pmatrix} 0 & 1 & 0\\ 0 & 0 & 0\\ 0 & 0 & -\zeta\end{pmatrix}\begin{pmatrix} u\\ v\\ w\end{pmatrix} + \begin{pmatrix} uv+v^2-vw/\zeta-\zeta uw\\ -\zeta uv-\zeta v^2+vw-\zeta vw\\ \zeta uv+\zeta v^2-vw-\zeta w^2\end{pmatrix}. \tag{2.6}$$

Note that $u-v$ plane is associated with a pair of zero eigenvalues, while the w axis corresponds to the eigenvalue $-\zeta$. Thus, there exists a smooth stable manifold $W^s(e_0)$ and center manifold $W^c(e_0)$. A center manifold at e_0 can be locally represented as:

$$W^c(e_0)=\{(u, v, w) \mid w=g(u, v),\ |u|<\delta,\ |v|<\delta,\ g(0)=Dg(0)=0\}$$

for δ sufficiently small, where g can be computed as a Taylor expansion up to a certain order to obtain the desired degree of accuracy, and the dynamics of (2.6) restricted to the center manifold is given by the first two equations in (2.6) with w replaced by $g(u, v)$. Note that g must have neither a constant nor a linear term, so we can compute the quadratic terms of g and get an approximation to the center manifold

$$w=\left(1-\frac{1}{\zeta}\right)v^2+uv+O(3). \tag{2.7}$$

Substituting (2.7) into (2.6) we obtain a center manifold reduction up to order 3:

$$\begin{aligned}\dot{u} &= v + v^2 + uv - \zeta u^2 v + \left(1 - \frac{1}{\zeta} - \zeta\right) uv^2 + \left(\frac{1}{\zeta^2} - \frac{1}{\zeta}\right) v^3 + O(4),\\ \dot{v} &= -\zeta uv - \zeta v^2 + \left((1-\zeta)\, uv^2 + \left(2 - \frac{1}{\zeta} - \zeta\right)\right) v^3 + O(4).\end{aligned} \tag{2.8}$$

The second order terms in (2.8) can be simplified by using the normal form theorem and computing a normal form up to order 2. We know from *Guckenheimer and Holmes* [6] that

$$H_2 = span\left\{\begin{pmatrix}x^2\\0\end{pmatrix}, \begin{pmatrix}xy\\0\end{pmatrix}, \begin{pmatrix}y^2\\0\end{pmatrix}, \begin{pmatrix}0\\x^2\end{pmatrix}, \begin{pmatrix}0\\xy\end{pmatrix}, \begin{pmatrix}0\\y^2\end{pmatrix}\right\},$$

$$L_J(H_2) = span\left\{\begin{pmatrix}-2xy\\0\end{pmatrix}, \begin{pmatrix}y^2\\0\end{pmatrix}, \begin{pmatrix}x^2\\-2xy\end{pmatrix}, \begin{pmatrix}xy\\-y^2\end{pmatrix}\right\},$$

and one choice of G_2 is given by

$$G_2 = span\left\{\begin{pmatrix}0\\x^2\end{pmatrix}, \begin{pmatrix}0\\xy\end{pmatrix}\right\}.$$

For the system (2.8), if we choose the near-identity transformation

$$\begin{pmatrix}u\\v\end{pmatrix} = \begin{pmatrix}x\\y\end{pmatrix} + \begin{pmatrix}\dfrac{1-\zeta}{2}\, x^2 + xy\\ -\zeta xy\end{pmatrix}, \tag{2.9}$$

i.e.,

$$\tilde{h}(x, y) = \begin{pmatrix}\dfrac{1-\zeta}{2}\, x^2 + xy\\ -\zeta xy\end{pmatrix},$$

then (2.8) can be transformed into the normal form

$$\begin{aligned}\dot{x} &= y + O(3),\\ \dot{y} &= -\zeta xy + O(3).\end{aligned} \tag{2.10}$$

We will be interested in studying perturbations of (2.10) which then represent the different types of dynamics that can occur for the full system (2.4) near the bifurcation.

Note that (2.10) is a degenerate case of (1.2) since the corresponding coefficient a of x^2 term is zero (see Section 1). When we compute a normal form of (2.10) up to order 3, we get the system

$$\dot{x} = y + O(4),$$
$$\dot{y} = -\zeta xy + \tfrac{1}{2}\zeta(\zeta - 1)\, x^2 y + O(4),$$

which is again a degenerate case of the normal form (1.4) for $\alpha = 0$. Since system (1.4) has a local codimension three bifurcation, our system (2.10) undergoes a bifurcation of codimension greater than or equal to three.

This completes the proof.

These degeneracies indicate that it will be extremely difficult to conduct a complete bifurcation analysis of (2.10). However, in this article we do not attempt to study all possible perturbations of (2.10). In fact, our biological considerations restrict the variables and parameters to be in a certain region. In other words, not all unfoldings will produce biologically feasible solutions. For example, note that in the original system (2.2) the region (2.3) is invariant, which implies that $y \geqslant 0$ should be invariant for the simplified system (2.10), so we must not introduce any term that produces solutions with $y(0) > 0$ but $y(\bar{t}) < 0$ for some $\bar{t} > 0$. Under these considerations, we will only look for a specific unfolding in (2.10) to capture some dynamics of the original system in terms of the simpler system in normal form. In particular, we want to find an unfolding that gives rise to limit cycles and homoclinic orbits since we expect these dynamics based on our numerical studies of the original system.

3. UNFOLDING ANALYSIS AND HOMOCLINIC BIFURCATION

When considering unfolding of systems of the form (2.10), one usually adds terms in the y equation only (see (1.3) and (1.5)). However, due to our biological considerations, all of these unfoldings will exclude the possibilities of limit cycles and homoclinic orbits. The reason for this is that the equilibria of such perturbed systems satisfy $y = 0$, and hence any periodic orbits spiraling around the equilibria will enter the lower half plane $y < 0$, which is not biologically feasible for our system (2.10). Therefore, there should be an unfolding term in the x equation in order to produce the appropriate dynamics.

We introduce the following unfolding of the system (2.10):

$$\begin{aligned} \dot{x} &= \sigma_1 x + y, \\ \dot{y} &= (\sigma_2 - \sigma_1)\, y + \alpha x^2 - \zeta xy. \end{aligned} \tag{3.1}$$

Here σ_1, σ_2, and α are small parameters, $\alpha \geqslant 0$. It is easy to verify that $y \geqslant 0$ remains invariant under the unfolding. We first consider the case when α is a fixed positive constant. We rescale by letting

$$x \to \frac{\alpha}{\zeta^2} x, \qquad y \to \frac{\alpha^2}{\zeta^3} y, \qquad t \to \frac{\zeta}{\alpha} t, \qquad \sigma_1 \to \frac{\alpha}{\zeta} \mu_1, \qquad \sigma_2 \to \frac{\alpha}{\zeta} \mu_2$$

to obtain a transformed system of (3.1):

$$\begin{aligned} \dot{x} &= \mu_1 x + y, \\ \dot{y} &= (\mu_2 - \mu_1)\, y + x^2 - xy. \end{aligned} \tag{3.2}$$

μ_1 and μ_2 are new parameters. System (3.2) has two equilibria $E_0 = (0, 0)$ and $E^* = (x^*, y^*)$, where

$$x^* = \frac{\mu_1(\mu_2 - \mu_1)}{1 + \mu_1}, \qquad y^* = \frac{\mu_1^2(\mu_1 - \mu_2)}{1 + \mu_1}.$$

For illustration we restrict our attention to the parameter region $\mu_2 \leqslant \mu_1$.

THEOREM 3.1. *A Hopf bifurcation occurs along the curve* $H = \{(\mu_1, \mu_2) \mid \mu_2 = -\mu_1^2, \mu_1 > 0\}$, *and the bifurcation is supercritical.*

Proof. Note that $x^* < 0$, $y^* > 0$ for $\mu_2 < \mu_1$, $\mu_1 \geqslant 0$. Hence E^* is in the interior of the half plane $y \geqslant 0$. E_0 is a saddle for all $\mu_2 < \mu_1$, $\mu_1 > 0$. The Jacobian at E^* is

$$A = \begin{pmatrix} \mu_1 & 1 \\ \dfrac{(2 + \mu_1)\, \mu_1(\mu_2 - \mu_1)}{1 + \mu_1} & \dfrac{\mu_2 - \mu_1}{1 + \mu_1} \end{pmatrix}.$$

Since

$$\operatorname{trace}(A) = \frac{\mu_1^2 + \mu_2}{1 + \mu_1} \qquad \text{and} \qquad \det(A) = \mu_1(\mu_1 - \mu_2),$$

we see that E^* is stable for $\mu_2 < -\mu_1^2$ and unstable for $\mu_2 > -\mu_1^2$. Thus, for each fixed μ_1, the roots of the characteristic equation cross the imaginary axis when μ_2 crosses $-\mu_1^2$ from left to right. It is easy to check that this crossing is transversal. We conclude that a Hops bifurcation occurs along the curve H.

To study the stability of the Hopf bifurcation, we first change coordinates to bring the point E^* to the origin and consider the system (3.2) with $\mu_2 = -\mu_1^2$. Letting $\bar{x} = x - x^*$, $\bar{y} = y - y^*$, we obtain

$$\begin{aligned} \dot{\bar{x}} &= \mu_1 \bar{x} + \bar{y}, \\ \dot{\bar{y}} &= -\mu_1^2(2 + \mu_1)\, \bar{x} - \mu_1 \bar{y} + \bar{x}^2 - \bar{x}\bar{y}. \end{aligned}$$

Then using the linear transformation

$$\begin{pmatrix} \bar{x} \\ \bar{y} \end{pmatrix} = T \begin{pmatrix} u \\ v \end{pmatrix},$$

where

$$T = \begin{pmatrix} 1 & 0 \\ -\mu_1 & -\mu_1 \sqrt{1+\mu_1} \end{pmatrix}$$

is the matrix of real and imaginary parts of the eigenvectors of the eigenvalues $\lambda = \pm i\mu_1 \sqrt{1+\mu_1}$, we obtain the system in "standard form":

$$\dot{u} = -\mu_1 \sqrt{1+\mu_1}\, v + f(u, v),$$
$$\dot{v} = \mu_1 \sqrt{1+\mu_1}\, u + g(u, v),$$

where

$$f = 0, \qquad g = -\frac{\sqrt{1+\mu_1}}{\mu_1} u^2 - uv.$$

The stability of the Hopf bifurcation is determined by the sign of the coefficient C which is given by the formula

$$C = \frac{1}{16}[f_{uuu} + f_{uvv} + g_{uuv} + g_{vvv}] + \frac{1}{16\omega}[f_{uv}(f_{uu} + f_{vv})$$
$$- g_{uv}(g_{uu} + g_{vv}) - f_{uu}g_{uu} + f_{vv}g_{vv}],$$

where $\omega = \mu_1 \sqrt{1+\mu_1}$ (cf. [6]). It is easy to verify that in our case

$$C = -\frac{1}{8\mu_1^2} < 0,$$

so that the bifurcation is *supercritical* and we have a family of stable periodic orbits for $\mu_2 > -\mu_1^2$ and close to H.

This completes the proof.

Let

$$\Omega = \{(\mu_1, \mu_2) \mid -2\mu_1^2 < \mu_2 < 0, \mu_1 > 0\}.$$

Then $H \subset \Omega$. It can be shown that, for $(\mu_1, \mu_2) \in \Omega$, $(\operatorname{trace}(A))^2 - 4 \det(A) < 0$, and hence E^* is a focus. Using arguments as in the analysis of Takens–Bogdanov's equations (cf. [1, Section 7.3]) we suspect the existence of global bifurcations.

THEOREM 3.2. *A homoclinic bifurcation occurs along the curve*

$$HL = \{(\mu_1, \mu_2) \mid \mu_2 = -\tfrac{6}{7}\mu_1^2 + O(\mu_1^3), \mu_1 > 0\}.$$

Proof. In order to find the homoclinic orbit of (3.2), we set

$$x \to \varepsilon^2 x, \qquad y \to \varepsilon^3 y, \qquad \mu_1 \to \varepsilon, \qquad \mu_2 \to -\varepsilon^2 v, \qquad t \to \frac{t}{\varepsilon}, \tag{3.3}$$

where ε and v are new parameters. Then (3.2) becomes

$$\begin{aligned} \dot{x} &= x + y, \\ \dot{y} &= -y + x^2 - \varepsilon(vy + xy). \end{aligned} \tag{3.4}$$

For $\varepsilon = 0$, (3.4) is a Hamiltonian system with Hamiltonian

$$H(x, y) = \frac{y^2}{2} + xy - \frac{x^3}{3}. \tag{3.5}$$

The phase portrait of (3.4) with $\varepsilon = 0$ is shown in Fig. 2. The separatrix cycle $\Gamma_0 \cup \{0\}$ shown in Fig. 2 corresponds to $H(x, y) = 0$; i.e., it is represented by motions on the curves defined by

$$y_{\pm}(x) = -x \pm \frac{\sqrt{3}}{3} x \sqrt{3 + 2x}, \qquad -\frac{3}{2} \leqslant x \leqslant 0.$$

Let $\gamma_0(t) = (x_0(t), y_0(t))$ be the solution on Γ_0, and let

$$\begin{aligned} \mathbf{f}(\gamma_0(t)) &= \begin{pmatrix} f_1(\gamma_0(t)) \\ f_2(\gamma_0(t)) \end{pmatrix} = \begin{pmatrix} x_0(t) + y_0(t) \\ -y_0(t) + x_0^2(t) \end{pmatrix}, \\ \mathbf{g}(\gamma_0(t), v) &= \begin{pmatrix} g_1(\gamma_0(t), v) \\ g_2(\gamma_0(t), v) \end{pmatrix} = \begin{pmatrix} 0 \\ -(v + x_0(t))\, y_0(t) \end{pmatrix}. \end{aligned} \tag{3.6}$$

We prove the existence of homoclinic orbits using Melnikov's method. To compute the Melnikov function

$$M(v) = \int_{-\infty}^{\infty} \mathbf{f}(\gamma_0(t)) \wedge \mathbf{g}(\gamma_0(t), v)\, dt,$$

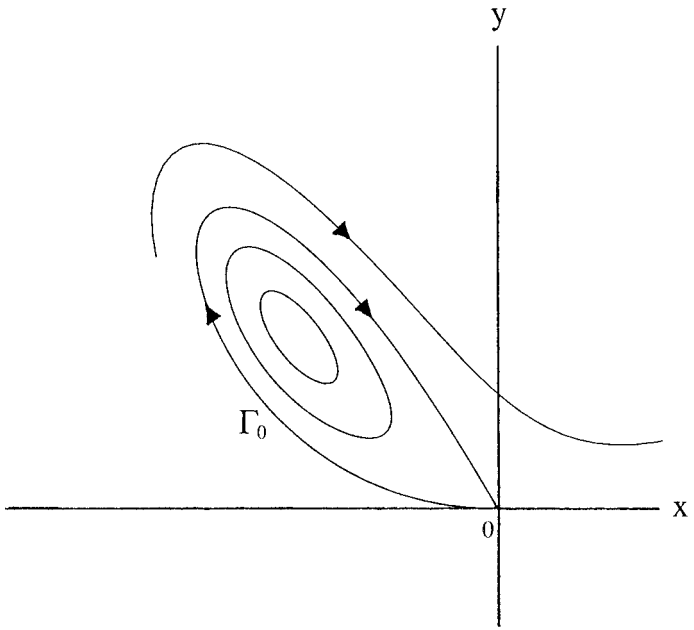

FIG. 2. The phase portraits of (3.4) with $\varepsilon = 0$.

where the wedge product of two vectors $\mathbf{u}$ and $\mathbf{v} \in \mathbf{R}^2$ is defined as $\mathbf{u} \wedge \mathbf{v} = u_1 v_2 - v_1 u_2$, we use (3.6) and the fact that along trajectories of (3.4) $dt = dx/\dot{x} = dx/f_1(\gamma_0)$ to obtain

$$
\begin{aligned}
M(v) &= \int_{-\infty}^{\infty} f_1(\gamma_0(t))\, g_2(\gamma_0(t), v)\, dt \\
&= \int_{-3/2}^{0} g_2(x, y_-(x), v)\, dx - \int_{-3/2}^{0} g_2(x, y_+(x), v)\, dx \\
&= \int_{-3/2}^{0} (v + x)(y_+(x) - y_-(x))\, dx \\
&= \frac{2\sqrt{3}}{3} \int_{-3/2}^{0} (v + x)\, x \sqrt{3 + 2x}\, dx \\
&= \frac{6}{35}(6 - 7v).
\end{aligned}
$$

We see that $M(v) = 0$ if and only if $v = 6/7$, and $M_v(6/7) \neq 0$. Thus, according to results in [1, see Theorem 4.5.3] for all sufficiently small $\varepsilon \neq 0$, there is a $v_\varepsilon = 6/7 + O(\varepsilon)$ such that the system (3.4) with $v = v^* = 6/7 + O(\varepsilon)$ has a

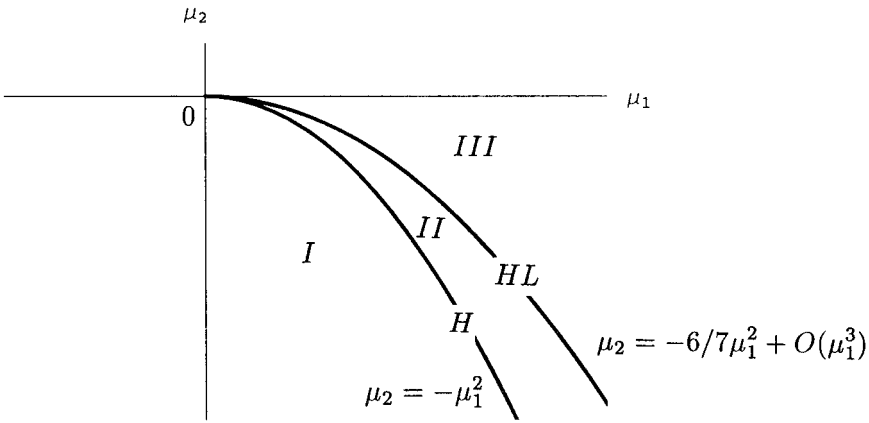

FIG. 3. The bifurcation diagram for the system (3.2) in the (μ_1, μ_2) plane. H and HL denote the curves for Hopf bifurcation and homoclinic bifurcation, respectively.

homoclinic orbit Γ_ε with the saddle at the origin in an ε-neighborhood of Γ_0. Using (3.3) ($\mu_1 = \varepsilon$, $\mu_2 = -\varepsilon^2 v$) we obtain the bifurcation curve HL for the system (3.2)

$$\mu_2 = -6/7\mu_1^2 + O(\mu_1^3), \qquad \mu_1 > 0. \tag{3.7}$$

Thus, for all sufficiently small $\mu_1 > 0$, the system (3.2) has a homoclinic orbit Γ_μ with $\mu = (\mu_1, \mu_2)$ on HL and the saddle at the origin. Note that the curve (3.7) lies to the right of the curve for Hopf bifurcation H which has the equation $\mu_2 = -\mu_1^2$, $\mu_1 > 0$.

This completes the proof.

Our knowledge so far leads to the bifurcation diagram for the system (3.2) shown in Fig. 3. The following result describes the number of periodic orbits for given μ_1 and μ_2.

THEOREM 3.3. *For sufficiently small μ_1 and μ_2,* (i) *there is a unique limit cycle in the region $-\mu_1^2 < \mu_2 < \frac{6}{7}\mu_1^2$, the limit cycle shrinks to the stable focus as (μ_1, μ_2) tends to H, and it tends to the homoclinic loop as (μ_1, μ_2) tends to HL;* (ii) *there are no periodic orbits in the regions $\mu_2 < -\mu_1^2$ (near H) and $\mu_2 > -\frac{6}{7}\mu_1^2$ (near HL).*

Proof. Let $P(x, y, \mu_2)$, $Q(x, y, \mu_2)$ denote the right hand side of the x and y equation in (3.2), respectively. Note that, for each fixed μ_1,

$$\det \begin{pmatrix} P & Q \\ P_{\mu_2} & Q_{\mu_2} \end{pmatrix} = \mu_1 xy + y^2 > 0, \tag{3.8}$$

if μ_1 is small. Thus (3.2) defines a *one-parameter family of rotated vector fields* (see [7]). Note that Γ_μ ($\mu \in HL$) is negatively oriented (as t increases, it moves clockwise). Also note that the trace of the Jacobian of (3.2) at E_0 (on the curve HL) is $-\mu_1^2 < 0$, and hence Γ_μ is an ω-limit set for nearby points in the interior of Γ_μ (cf. [6, Section 6.1]). Using results in [7, Theorem 4.6.3] we know that Γ_μ generates a unique limit cycle on its interior as μ_2 decreases. Since these limit cycles are bounded by Γ_μ and the parameter μ_2 is also bounded, from *Perko's Planar Termination Principle* (see [7]) we know that the maximal, one-parameter (μ_2) family of limit cycles terminates at a critical point or a separatrix cycle. Since the limit cycle for each μ_2, $-\mu_1^2 < \mu_2 < -6/7\mu_1^2$ is stable and negatively oriented, it shrinks continuously as μ_2 decreases (or expands continuously as μ_2 increases). It is easy to show that this family of limit cycles contains the branch of periodic solutions from the Hopf bifurcation. The limit cycle must shrink to E^* when μ_2 decreases to $-\mu_1^2$, since otherwise E^* will be unstable for some $\mu_2 < -\mu_1^2$ which is a contradiction. This also shows that E^* is a stable focus for $(\mu_1, \mu_2) \in H$. It is clear that the limit cycle must expand to Γ_μ when μ_2 increases to $-6/7\mu_1^2$. This completes the proof of part (i).

To prove part (ii), we let L be the segment connecting E_0 and E^*:

$$L = \left\{ (x, y) \;\middle|\; \frac{\mu_1(\mu_2 - \mu_1)}{1 + \mu_1} < x < 0,\ y = -\mu_1 x \right\}.$$

Note that E_0 is a saddle and E^* is a focus which is stable when $\mu_2 < -\mu_1^2$ (near H) and unstable when $\mu_2 > -\frac{6}{7}\mu_1^2$ (near HL). Hence any periodic orbit of (3.2), if it exists, must cut the segment L. We know from part (i) that if $(\mu_1, \mu_2) \in (H \cup HL)$, then the system (3.2) has no periodic orbits, and any positive trajectory γ starting from the point $p \in L$ is a contracting spiral if $(\mu_1, \mu_2) \in H$ or an expanding spiral if $(\mu_1, \mu_2) \in HL$. For (μ_1, μ_2) below H (or above HL), we can find $(\mu_1, \bar{\mu}_2) \in H$ (or $\in HL$). Let γ and $\bar{\gamma}$ denote the two positive trajectories starting from the same point $p \in L$ and corresponding to (μ_1, μ_2) and $(\mu_1, \bar{\mu}_2)$, respectively. Then $\bar{\gamma}$ is a contracting (expanding) spiral. Note that (3.8) implies that at each ordinary point of (3.2), where $P^2 + Q^2 \neq 0$, the field vector rotates counterclockwise as μ_2 increases. Thus, γ must be located entirely inside (outside) $\bar{\gamma}$. This means that γ cannot be a closed orbit.

This completes the proof.

We now look at some numerical results. Computations of the system (3.2) with Ermentrout's program XPPAUT show that the equilibrium E^* loses its stability for $\mu_2 > -\mu_1^2$ and $(\mu_1, \mu_2) \in \Omega$ (see Fig. 4). Here we have chosen $\mu_1 = 0.5$ for all plots in Fig. 4. The plot in Fig. 4a shows that E^* is a stable focus for $\mu_2 = -0.3$ (so that (μ_1, μ_2) is in the region I). Note that the solution with initial data $y(0) > 0$ remains in the upper half plane.

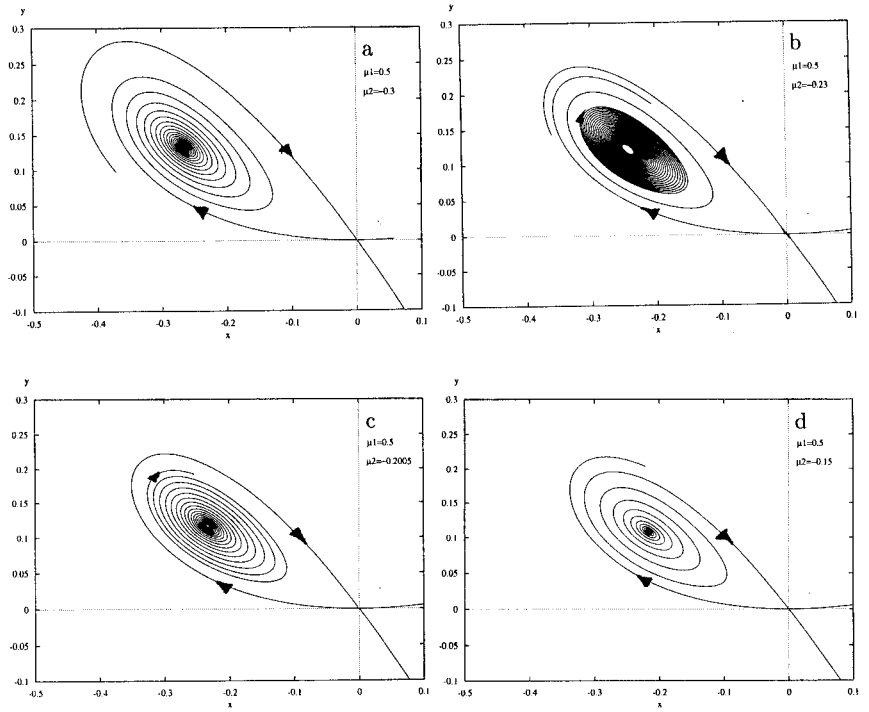

FIG. 4. Numerical integration of the system (3.2) according to XPPAUT. μ_1 and μ_2 have been chosen such that (μ_1, μ_2) is in the region *I*, *II*, *HL* and *III*, respectively. These regions are as in Fig. 3.

Figure 4b is for $\mu_2 = -0.23$, and hence $(\mu_1, \mu_2) \in II$. We see that E^* is unstable, and there is a unique ω-limit cycle. We have observed that the limit cycle expands as μ_2 increases until $\mu_2 \approx -0.2005$, at which time the limit cycle hits the saddle point E_0 and a homoclinic orbit occurs (see Fig. 4c). Hence $(\mu_1, \mu_2) = (0.5, -0.2005) \in HL$. When $\mu_2 = -0.15$; i.e., $(\mu_1, \mu_2) \in III$ (see Fig. 4d), we see that the stable and unstable manifolds of the saddle point E_0 change their relative positions comparing with the case of $(\mu_1, \mu_2) \in II$. It is clear that our analytical results are confirmed by these numerical calculations.

Notice that both Theorems 3.1 and 3.2 consider parameter regions in which $\mu_1 > 0$. For $\mu_1 < 0$ the dynamics are much simpler, and we will not discuss them further. We remark that for each fixed α, a bifurcation diagram for the system (3.1) in the (σ_1, σ_2) plane can be obtained using the formula $\sigma_i = \frac{\alpha}{\zeta}\mu_i$, $(i = 1, 2)$. The corresponding curves are similar to those in the (μ_1, μ_2) plane given in Fig. 4 (scaled by α/ζ). When α varies we get a surface of Hopf bifurcation and a surface of homoclinic bifurcation for the system (3.1) in the $(\sigma_1, \sigma_2, \alpha)$ space (see Fig. 5).

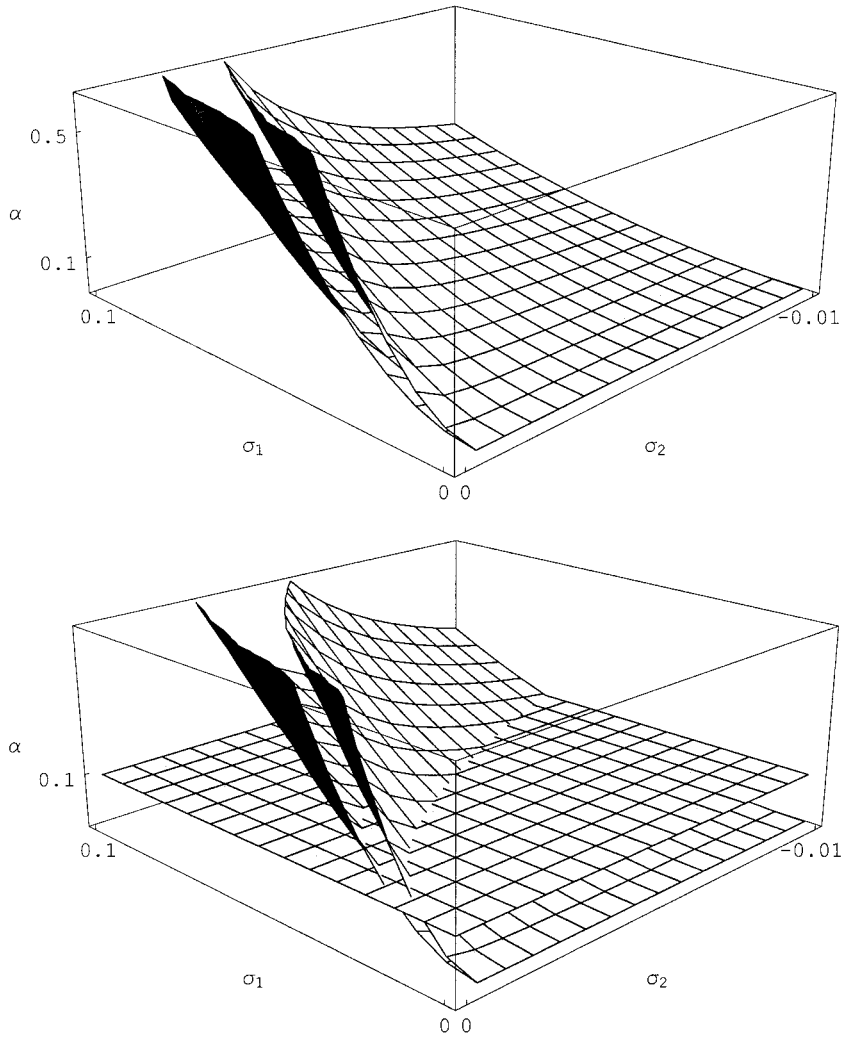

FIG. 5. The bifurcation diagram for the system (3.1) in the $(\sigma_1, \sigma_2, \alpha)$ space. The top graph shows two surfaces which denote Hopf bifurcation (upper) and homoclinic bifurcation (lower), respectively. The bottom graph shows the two bifurcation curves H and HL for a fixed value of $\alpha = 0.1$ (the curves are given by the intersections of the surfaces with the plane $\alpha = 0.1$).

DISCUSSION

In this paper we studied possible complex dynamics that can occur in an *SIQR* epidemic model for childhood diseases under small perturbation. We first identify a bifurcation point of the vector fields associated with the model. This occurs at $p = q = z = 0$ for parameter values $v = 0$, $\theta = 1$ (see (2.4)). We then compute a center manifold reduction and a normal form which appears to be highly degenerate (see (2.10)). The degeneracy indicates the existence of bifurcations of codimension greater than two. We proceed to look for a specific unfolding of the normal form to capture appropriate dynamics of the original system under certain biological constraints on the state space. We find a specific unfolding which produces limit cycles and homoclinic bifurcations, and construct a bifurcation diagram in the parameter space. These findings provide an analytic understanding of the numerical observations in the *SIQR* model. We also conduct some numerical calculations which confirm our analytical results.

Although the unfolded system may not correspond to the original model equations, it represents the different dynamics the model may have under small perturbations. Ideally, one would like to know how the parameters of the unfolded system (3.2) are related to the parameters in the original system (2.2) or (2.1). This is a nontrivial task due to the series of nonlinear transformations. Our preliminary results show that correspondence between a perturbation of the original system (2.1) and the simplified system (3.2) can be established under certain circumstances. These results will be included in Wu's thesis. More explicitly, the incorporation (as perturbations) of factors such as migration of various epidemiological classes, partial immunity, disease-induced death, relapse of the disease, etc. into the model allows for the possibility of the normal form reduction (3.1) and the simplified system (3.2). Moreover, when the basic reproductive number $\mathscr{R}_0$ is close to one, the corresponding parameters μ_1 and μ_2 in (3.2) are small. That is, in the perturbed *SIQR* model, not only an endemic equilibrium may occur near the critical value of $\mathscr{R}_0 = 1$, but also the system can exhibit complex disease dynamics corresponding to the homoclinic bifurcation.

REFERENCES

1. R. I. Bogdanov, Versal deformations of a singular point on the plane in the case of zero eigenvalues, *Funct. Anal. Appl.* **9** (1975), 144–145.
2. S.-N. Chow, C. Li, and D. Wang, "Normal Forms and Bifurcation of Planar Vector Fields," Cambridge University Press, Cambridge, UK, 1994.
3. E. J. Doedel, Auto: a program for the automatic bifurcation analysis of autonomous systems, *Congr. Numer.* **30** (1981), 265–284.

4. F. Dumortier, R. Roussarie, J. Sotomayor, and H. Zoladek, "Bifurcations of Planar Vector Fields," Lecture Notes in Mathematics, Vol. 1480, Springer-Verlag, Berlin/Heidelberg/New York, 1991.
5. Z. Feng and H. Thieme, Recurrent outbreaks of childhood diseases revisited: The impact of isolation, *Math. Biosci.* **128** (1995), 93–130.
6. J. Guckenheimer and P. J. Holmes, "Nonlinear Oscillations, Dynamical Systems, and Bifurcations of Vector Fields," Applied Mathematical Sciences, Vol. 42, Springer-Verlag, New York, 1983.
7. L. Perko, "Differential Equations and Dynamical Systems," Texts in Applied Mathematics, Vol. 7, Springer-Verlag, New York, 1996.
8. S. Wiggins, "Introduction to Applied Nonlinear Dynamical Systems and Chaos," Texts in Applied Mathematics, Vol. 2, Springer-Verlag, New York, 1990.